

# Equation of state of two-dimensional $^3\text{He}$ at zero temperature

M. Nava, A. Motta, and D.E. Galli

*Dipartimento di Fisica, Università degli Studi di Milano, via Celoria 16, 20133 Milano, Italy*

E. Vitali

*IOM-CNR DEMOCRITOS National Simulation Center, via Beirut 2-4, 34014 Trieste, Italy and  
Dipartimento di Fisica, Università degli Studi di Milano, via Celoria 16, 20133 Milano, Italy*

S. Moroni

*IOM-CNR DEMOCRITOS National Simulation Center, via Beirut 2-4, 34014 Trieste, Italy*

(Dated: April 22, 2022)

We have performed a Quantum Monte Carlo study of a two-dimensional bulk sample of interacting  $1/2$ -spin structureless fermions, a model of  $^3\text{He}$  adsorbed on a variety of preplated graphite substrates. We have computed the equation of state and the polarization energy using both the standard fixed-node approximate technique and a formally exact methodology, relying on bosonic imaginary-time correlation functions of operators suitably chosen in order to extract fermionic energies. As the density increases, the fixed-node approximation predicts a transition to an itinerant ferromagnetic fluid, whereas the unbiased methodology indicates that the paramagnetic fluid is the stable phase until crystallization takes place. We find that two-dimensional  $^3\text{He}$  at zero temperature crystallizes from the paramagnetic fluid at a density of  $0.061 \text{ \AA}^{-2}$  with a narrow coexistence region of about  $0.002 \text{ \AA}^{-2}$ . Remarkably, the spin susceptibility turns out in very good agreement with experiments.

PACS numbers:

## I. INTRODUCTION

A quasi-two-dimensional (2d) bulk  $^3\text{He}$  sample at zero temperature is a very fascinating scenario to explore the physics of strongly correlated Fermions. The liquid phase can be experimentally realized over a wide range of densities by adsorbing  $^3\text{He}$  on a variety of preplated graphite substrates.<sup>1-3</sup> Heat capacity and magnetization measurements show that the system displays a nearly perfect Fermi liquid behavior, with the effective mass  $m^*$  and the enhancement of the spin susceptibility  $\chi/\chi_0$  increasing with the density. These observations, consistent with a divergence of  $m^*$  near the freezing density, have been interpreted<sup>3</sup> as a signature of a Mott transition leading to an insulating crystal. However theoretical approaches<sup>4</sup> suggest that the singularity of  $m^*$  and freezing could not have the same origin, and indeed the freezing density (as well as the magnetic properties of the solid<sup>5</sup>, and even the presence of a possible intermediate phase of a uniform gas of vacancies<sup>6</sup>) is influenced by the preplated substrate. In order to characterize the sole effect of correlations, it is therefore of particular interest to study the ideal, strictly two-dimensional liquid on the verge of crystallization, in the absence of any external potential. The measured properties of the fluid phase, on the other hand, appear to be largely independent of the substrate, so that they can be directly compared to the calculated properties of the ideal model<sup>7</sup>.

From the theoretical side, such a system provides a severe test case for microscopic calculations<sup>8</sup>, because of the strong correlations attained at high densities. We thus resort to quantum Monte Carlo (QMC) simulation,

a powerful tool to study strongly interacting systems, and we calculate the ground-state energy per particle  $e = \frac{E}{N}$  of the 2d  $^3\text{He}$  liquid at zero temperature as a function of the number density  $\rho$  and the spin polarization  $\zeta$ .

The dependence of the energy on the spin polarization is in general very weak in strongly correlated fluids<sup>9-12</sup>. The so-called fixed-node (FN) approximation<sup>13</sup>, used in most QMC calculations, has been argued to give a significant bias in the polarization energy of three-dimensional liquid  $^3\text{He}$ <sup>10</sup> at high density.

We thus perform our study going also beyond the FN level, following a formally exact method<sup>12</sup>, slightly different from the well known transient estimate (TE) technique<sup>14</sup>. Briefly, we perform simulations relying on the basic Hamiltonian in an enlarged, unphysical space of states of any symmetry, including those with Fermi and Bose statistics. The ground state energy of the physical fermionic  $^3\text{He}$  is considered as an excitation energy of the absolute bosonic ground state, which is sampled exactly with QMC. In this approach one trades the sign problem faced by TE<sup>14</sup> for the analytic continuation needed to extract excitation energies from suitable imaginary-time correlation functions. A mixed approach, devised to ease detection of the asymptotic convergence of TE by a Bayesian analysis of imaginary-time correlation functions, was proposed by Caffarel and Ceperley<sup>15</sup>.

In fact a previous FN QMC calculation exists<sup>16</sup>, but it is limited to low densities and only considers the paramagnetic fluid phase. In particular, the accuracy of the FN approximation in the high density regime is questionable<sup>10</sup>.

We find indeed that the FN level of the theory and

the exact calculation predict a qualitatively different behavior: within FN the system becomes ferromagnetic well before crystallization takes place upon increasing the density, whereas the unbiased calculation shows that the spin polarization of the fluid is preempted by freezing, as observed experimentally. From the estimated curve  $e(\zeta)$  we obtain a spin susceptibility enhancement in quantitative agreement with the available measurements.

## II. QMC SIMULATION

We simulate  $N$  particles with the mass  $m_3$  of  ${}^3\text{He}$  atoms, interacting with the HFDHE2 pair potential<sup>17</sup> in periodic boundary conditions. The simulation box, of area  $\Omega$ , is a square of side  $L$  for the liquid phase; for the solid it is a rectangle which accommodates a triangular lattice. The Hamiltonian is

$$\hat{H} = -\frac{\hbar^2}{2m_3} \sum_{i=1}^N \nabla_i^2 + \sum_{i<j=1}^N v(\vec{r}_i - \vec{r}_j) \quad (1)$$

If the particles obey Bose statistics, projection QMC methods<sup>18–20</sup> provide unbiased estimates of the ground-state energy and other physical observables. This is made possible by the formal similarity between Schrödinger equation in imaginary time and the differential equation governing a diffusion process in probability theory. Such a useful possibility however drops down when Fermi statistics enters the game because of the well known sign problem<sup>14</sup>.

### A. Fixed-Node approach

The most commonly used approach in the QMC simulation of Fermions is the fixed-node approximation<sup>13</sup>, which stochastically solves the imaginary-time Schrödinger equation subject to the boundary conditions implied by the nodal structure of a given trial function  $\Psi_T$ . This approach gives a rigorous upper bound to the ground state energy, which often turns out to be extremely accurate.

For a given spin polarization, i.e. considering  $N_\uparrow$  spin-up and  $N_\downarrow = N - N_\uparrow$  spin-down  ${}^3\text{He}$  atoms,  $\Psi_T$  is chosen of the form

$$\Psi_T(\mathcal{R}) = \mathcal{D}(\mathcal{R}_\uparrow)\mathcal{D}(\mathcal{R}_\downarrow)\Psi_J(\mathcal{R})\chi_\zeta \quad (2)$$

where  $\mathcal{R} \equiv (\vec{r}_1, \dots, \vec{r}_N)$ ,  $\mathcal{R}_\uparrow \equiv (\vec{r}_1, \dots, \vec{r}_{N_\uparrow})$ ,  $\mathcal{R}_\downarrow \equiv (\vec{r}_{N_\uparrow+1}, \dots, \vec{r}_N)$ , and the whole dependence on the spin degrees of freedom is contained in  $\chi_\zeta$ , a spin eigenfunction for the given polarization

$$\zeta = \frac{N_\uparrow - N_\downarrow}{N} \quad , \quad (3)$$

The Jastrow factor,

$$\Psi_J(\mathcal{R}) = \prod_{i<j} \exp\left(-\frac{1}{2}u(|\vec{r}_i - \vec{r}_j|)\right), \quad (4)$$

describes pair correlations arising from the interaction potential; we use a simple pseudopotential of the McMillan form  $u(r) = (b/r)^5$ . Finally, the simplest form of the antisymmetric factors  $\mathcal{D}(\mathcal{R}_{\uparrow,\downarrow})$  is in the form of Slater Determinants of plane waves:

$$\mathcal{D}(\mathcal{R}_{\uparrow,\downarrow}) = \det\left(\left\{\exp(i\vec{k}_i \cdot \vec{r}_j)\right\}_{i,j}\right) \quad (5)$$

More accuracy in the FN results is achieved by introducing also backflow correlations<sup>21</sup> via quasi-particles vector positions:

$$\mathcal{D}(\mathcal{R}_{\uparrow,\downarrow}) = \det\left(\left\{\exp(i\vec{k}_i \cdot \vec{x}_j)\right\}_{i,j}\right) \quad (6)$$

$$\vec{x}_j \stackrel{\text{def}}{=} \vec{r}_j + \sum_{i \neq j=1}^N \eta(|\vec{r}_j - \vec{r}_i|)(\vec{r}_j - \vec{r}_i).$$

For the backflow correlation function  $\eta(r)$  we adopt the simple form:

$$\eta(r) = Ae^{-B(r-C)^2} \quad . \quad (7)$$

We will refer to the two choices respectively as plane waves fixed-node (PW-FN) and backflow fixed-node (BF-FN). For each density, the variational parameters  $b$ ,  $A$ ,  $B$  and  $C$  are optimized using correlated sampling<sup>22</sup> at  $\zeta = 0$ , and left unchanged at different polarizations.

Part of the bias related to the finite size of the simulated system arises from shell effects in the filling of single-particle orbitals<sup>23</sup>. This bias can be substantially reduced adopting twisted boundary conditions<sup>23</sup>, i.e. choosing  $\vec{k}$  appearing in (5) and (6) inside the set:

$$\vec{k}_{\vec{n}} = \frac{2\pi\vec{n} + \vec{\theta}}{L} \quad (8)$$

where  $\vec{n}$  is an integer vector,  $L$  is the side of the simulation box  $\Omega$  and  $\vec{\theta}$  is a *twist parameter*  $\theta_i \in [0, \pi]$  which, at the end of the calculations, is averaged over.

In the solid phase, quantum exchanges are strongly suppressed and the energy difference between a Fermionic and a Bosonic crystal is negligibly small for the purpose of locating the liquid-solid transition. We will therefore replace the energy of  ${}^3\text{He}$  with that of a fictitious bosonic Helium of mass  $m_3$ , which can be calculated exactly<sup>19,20,24</sup>. The small error incurred by such replacement is bound by the difference between the fermionic Fixed-Node (FN) energy and the unbiased bosonic energy. This difference, calculated<sup>25</sup> as a check at the melting density where it is expected to be largest, is indeed in the sub-milliKelvin range.

## B. Fermionic correlations approach

For the fluid phases the FN approximation may not be accurate enough, particularly at high density where correlations are stronger and the energy balance between different polarization states is more delicate. Indeed, a FN study of three-dimensional  $^3\text{He}$ , despite the use of sophisticated backflow correlations, strongly suggests that this is the case<sup>10</sup>. We thus perform calculations beyond the FN approximation, using a technique<sup>12</sup> which is in principle exact, albeit practically limited to moderate system sizes. The idea, in part related to the transient estimate formalism<sup>14,15</sup>, is that of formally viewing (1) as an operator acting inside the Hilbert space  $\mathcal{H}(N) \equiv (L^2(\Omega))^{\otimes N}$ , that is *forgetting* spin and statistics: one can use Quantum Monte Carlo to sample the lowest energy eigenfunction  $\psi_0(\mathcal{R})$  of  $\hat{H}$  among the states of any symmetry.

It is known<sup>26</sup> that  $\psi_0$  must share the *Bose symmetry* of the Hamiltonian, so that:

$$E_0^B \equiv \frac{\langle \psi_0 | \hat{H} \psi_0 \rangle_{\mathcal{H}(N)}}{\langle \psi_0 | \psi_0 \rangle_{\mathcal{H}(N)}} \quad (9)$$

is the Ground State energy of a fictitious system of  $N$  Bosons of mass  $m_3$  interacting via the potential  $v(r)$ .

The *bridge* that gives access to fermionic energies may be built up as follows: let us fix a spin polarization which is surely a good quantum number since the basic Hamiltonian is spin-independent. As discussed in Ref.12, if we are able to define an operator  $\hat{\mathcal{A}}_F$  such that, inside  $\mathcal{H}(N)$ ,

$$\psi_F(\mathcal{R}) = \left( \hat{\mathcal{A}}_F \psi_0 \right) (\mathcal{R}) \quad (10)$$

has *non-zero overlap* with the configurational part of any *exact fermionic* Ground State of  $\hat{H}$  for the given  $\zeta$ , we can define the *imaginary-time correlation function*:

$$\mathcal{C}_F(\tau) \equiv \frac{\langle \psi_0 | \left( e^{\tau \hat{H}} \hat{\mathcal{A}}_F^\dagger e^{-\tau \hat{H}} \right) \hat{\mathcal{A}}_F \psi_0 \rangle_{\mathcal{H}(N)}}{\langle \psi_0 | \psi_0 \rangle_{\mathcal{H}(N)}}, \quad \tau \geq 0 \quad (11)$$

which can be straightforwardly evaluated in a bosonic QMC simulation<sup>18,20,24</sup>. The lowest energy contribution in  $\mathcal{C}_F(\tau)$  provides the *exact gap* between the fermionic and the bosonic ground states of the two-dimensional Fermi liquid; this can be readily seen by formally expressing (11) on the basis  $\{\psi_n\}_{n \geq 0}$  of eigenvectors of  $\hat{H}$  corresponding to the eigenvalues  $\{E_n\}_{n \geq 0}$ :

$$\mathcal{C}_F(\tau) = \sum_{n=0}^{+\infty} e^{-\tau(E_n - E_0^B)} \frac{|\langle \hat{\mathcal{A}}_F \psi_0 | \psi_n \rangle|^2}{\langle \psi_0 | \psi_0 \rangle} \quad (12)$$

A quite natural choice<sup>12</sup> is to define  $\hat{\mathcal{A}}_F$  borrowing suggestions from the form of the trial wave function for the FN calculation, i.e.:

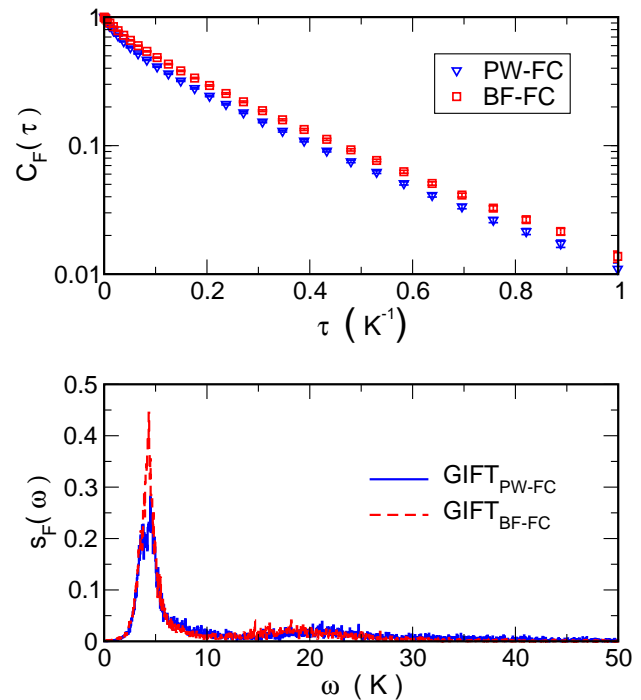


Figure 1: (Color online) Upper panel: Imaginary time correlation functions,  $\mathcal{C}_F(\tau)$ , corresponding to the two different choices of the operator in (13). Lower panel: reconstructed spectral functions  $s_F(\omega)$  obtained with the GIFT method.

$$\left( \hat{\mathcal{A}}_F \psi_0 \right) (\mathcal{R}) \stackrel{def}{=} \mathcal{D}(\mathcal{R}_\uparrow) \mathcal{D}(\mathcal{R}_\downarrow) \psi_0(\mathcal{R}) \quad (13)$$

where we can choose either the definition (5) of  $\mathcal{D}$  or the definition (6). We will refer to such choices simply as the plane waves fermionic correlations (PW-FC) and the backflow fermionic correlations (BF-FC). Naturally the final results for the Bose-Fermi gap should coincide within statistical uncertainties, and the actual comparison can be a good test for the robustness of the approach.

## III. ANALYTIC CONTINUATION

Once we have achieved a QMC evaluation of  $\mathcal{C}_F(\tau)$ , the information about the Bose-Fermi gap  $\Delta_{BF} = E_0 - E_0^B$  is contained in the resulting correlation functions. The results for  $\mathcal{C}_F(\tau)$  appear as simple smooth decreasing functions, whose values can be evaluated only in correspondence with a finite number of imaginary-time values, say  $\{\tau_0, \tau_1, \tau_2, \dots, \tau_l\}$ ; moreover the data are perturbed by unavoidable statistical uncertainties. The Bose-Fermi gap  $\Delta_{BF}$  is thus hidden inside the sets of limited and noisy data. How can we extract it? In the upper panel of Fig. 1 we show two imaginary time correlation functions  $\mathcal{C}_F(\tau)$ , respectively a PW-FC and a BF-FC, corresponding to the same spin polarization and twist parameter.

The long- $\tau$  tails of the two curves tend towards a linear behavior (in logarithmic scale) with the same slope, and this is a general feature shared by all the functions we have evaluated. This indicates that, because of the finite-size of the system (and selection rules on the total momentum), the fermionic spectrum has a significant gap, i.e. the lowest-energy term  $\exp(-\Delta_{BF}\tau)$  in the correlation function (12) appears to be quite well resolved with respect to contributions from higher fermionic energies. The difference between the two curves (in particular the rigid shift between their asymptotic tails) arises from the spectral weight of the Ground State contribution, which is higher when backflow correlations are taken into account, as expected.

In this favorable situation, the Bose-Fermi gap can be reliably extracted by simply fitting an exponential to the long-time tail of the correlation function.

This key result is strongly supported by a more sophisticated approach, which evaluates  $\Delta_{BF}$  by performing the full Laplace transform inversion of  $\mathcal{C}_F(\tau)$ , i.e. solving

$$\mathcal{C}_F(\tau) = \int_0^{+\infty} d\omega e^{-\tau\omega} s_F(\omega) \quad , \quad (14)$$

for the unknown *spectral function*  $s_F(\omega)$ . Recently a new method, the genetic inversion via falsification of theories (GIFT) method,<sup>27</sup> has been developed to face general inverse problems and in particular it has allowed to reconstruct the excitation spectrum of superfluid <sup>4</sup>He starting from QMC evaluations of the intermediate scattering function in imaginary-time<sup>27</sup>; the results were in close agreement with experimental data<sup>27</sup>. Moreover the method has allowed to extract also multiphonon energies with a good accuracy level. When applied to the two curves depicted in the upper panel of Fig. 1, we find the two spectral functions in the lower panel of Fig. 1; it is apparent that the lowest- $\omega$  peak is indeed well resolved from higher-energy contributions. Crucially, its position does not depend on the actual choice of the operator  $\hat{A}_F$ , and it is in excellent agreement with the smallest decay constant found by the simple exponential fit. The spectral weight instead is different, consistently with the differences between PW-FC and BF-FC.

In this work we adopt an implementation of the inversion via falsification of theories, detailed in the Appendix, which avoids the rather CPU-intensive genetic algorithms<sup>28</sup>. This is crucial in the present study, which involves an extremely large number of reconstructed spectra. Indeed, a single QMC simulation for a given density produces correlation functions pertaining to PW or BF operators, several spin polarizations, and 15 twist parameters in the irreducible wedge of the Brillouin zone of the simulation cell; on top of this, data are collected in several blocks, individually processed to obtain statistical uncertainties on the position of the lowest-energy peak.

Table I: The equations of state of <sup>3</sup>He for the paramagnetic fluid and the solid (solid lines in Figure 2) are of the form  $\alpha_1\rho + \alpha_2\rho^2 + \alpha_3\rho^3 + \alpha_4\rho^4 + \alpha_5\rho^5$ . This Table lists the values of the parameters  $\alpha_i$ , with lengths in  $\text{\AA}$ .

|            | liquid    | solid     |
|------------|-----------|-----------|
| $\alpha_1$ | 21.23782  | 57.35474  |
| $\alpha_2$ | -1344.413 | -2598.784 |
| $\alpha_3$ | 45093.37  | 58695.29  |
| $\alpha_4$ | -569306.0 | -532201.7 |
| $\alpha_5$ | 4383507   | 3063129   |

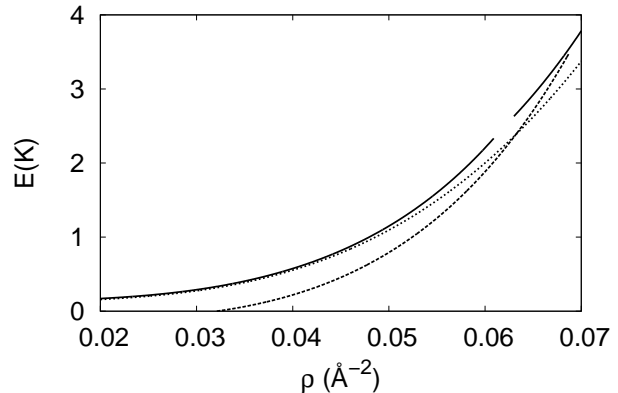


Figure 2: Equation of state of <sup>3</sup>He in two dimensions. Solid line (broken across the coexistence region): liquid and solid <sup>3</sup>He; dashed line: mass-3 boson fluid; dotted line: liquid <sup>3</sup>He, after Ref. 16. The latter is only reliable at low densities.

#### IV. RESULTS

We fit a fifth order polynomial to the density dependence of the energies of the triangular crystal and of the paramagnetic and the ferromagnetic fluids, listed in Table I. The resulting equation of state of two-dimensional <sup>3</sup>He is shown in Figure 2. With the fermionic correlations method, we find a transition between the paramagnetic fluid and the triangular crystal around  $\rho = 0.061 \text{ \AA}^{-2}$ , with a narrow coexistence of about  $0.002 \text{ \AA}^{-2}$ , while the ferromagnetic fluid is never stable (see Table II). The energy of the bosonic mass-3 liquid is also shown. This fictitious system, simulated to extract the PW-FC and BF-FC energies, crystallizes at  $\rho = 0.069 \text{ \AA}^{-2}$ . The freezing density of <sup>3</sup>He is considerably higher than the highest density simulated in Ref.16. Correspondingly, the equation of state given in Ref.16 is only reliable at relatively low density. In particular, while it is only slightly below our results for  $\rho \lesssim 0.045 \text{ \AA}^{-2}$  as a consequence of the difference of interparticle potential adopted<sup>29</sup>, it becomes (unphysically) even lower than the bosonic equation of state near the melting density, by an amount far larger than what could be due to the potential.

The treatment of the spin polarization state requires a special care<sup>9-12</sup>. In contrast to Ref.16, we find that the

Table II: Ground state energy of  $^3\text{He}$  in K, calculated by the FC method for the fluid phases and assumed to equal the bosonic energy for the solid phase.

|       | liquid $\zeta = 0$ | liquid $\zeta = 1$ | solid       |
|-------|--------------------|--------------------|-------------|
| 0.020 | 0.1707(18)         | 0.3218(25)         |             |
| 0.045 | 0.8168(86)         | 0.9075(86)         |             |
| 0.050 | 1.1500(81)         | 1.2123(88)         |             |
| 0.055 | 1.5972(93)         | 1.6574(91)         |             |
| 0.060 | 2.2069(68)         | 2.2493(54)         | 2.2506(54)  |
| 0.065 | 3.0065(73)         | 3.0359(45)         | 2.9195(26)  |
| 0.070 | 4.0644(33)         | 4.0915(34)         | 3.7878(35)  |
| 0.075 |                    |                    | 4.8728(44)  |
| 0.080 |                    |                    | 6.2445(35)  |
| 0.085 |                    |                    | 7.9589(39)  |
| 0.090 |                    |                    | 10.0661(46) |
| 0.095 |                    |                    | 12.6739(39) |
| 0.100 |                    |                    | 15.8536(45) |

BF-FN energy can be significantly higher than the unbiased Fermionic correlations (FC) energy. Starting from negligible values at low density, the BF-FN error quickly increases approaching the strongly correlated regime. As expected<sup>10</sup>, it is larger for the paramagnetic than for the ferromagnetic fluid. These findings are exemplified in Figure 3. The inadequacy of the BF-FN is striking in the phase diagram: Figure 4 shows that BF-FN incorrectly predicts a transition to a ferromagnetic fluid well before crystallization takes place. Such a transition is also evident from Figure 5, which shows the BF-FN results for the polarization energy  $e(\zeta)$  at various densities. The unbiased results, shown in Figure 6, display instead a paramagnetic behavior even in a metastable fluid phase well beyond the freezing density.

From the FC polarization energy  $e(\zeta)$  we can estimate the spin susceptibility enhancement  $\chi/\chi_0$ . Assuming a quadratic dependence over the whole polarization range, which is generally consistent with the data of Figure 6, we find an excellent agreement with the measured susceptibility. Figure 7 shows the comparison between the calculated  $\chi/\chi_0$  and the experimental data. We display only the results obtained in the second layer of  $^3\text{He}$  on graphite<sup>2</sup> since they extend to the highest density in the fluid phase, but experiments carried on with differently prepleated substrates lead to equivalent results in their respective density ranges. The agreement among the results obtained using different substrates induces us to expect that our ideal model actually captures the physical mechanisms underlying the behavior of  $\chi/\chi_0$ .

## V. CONCLUSIONS

We have calculated the equation of state and the polarization energy of  $^3\text{He}$  in two dimensions by means of an unbiased QMC method. The system crystallizes into a triangular lattice from the paramagnetic fluid at a density of  $0.061 \text{ \AA}^{-2}$ , with a narrow coexistence region of

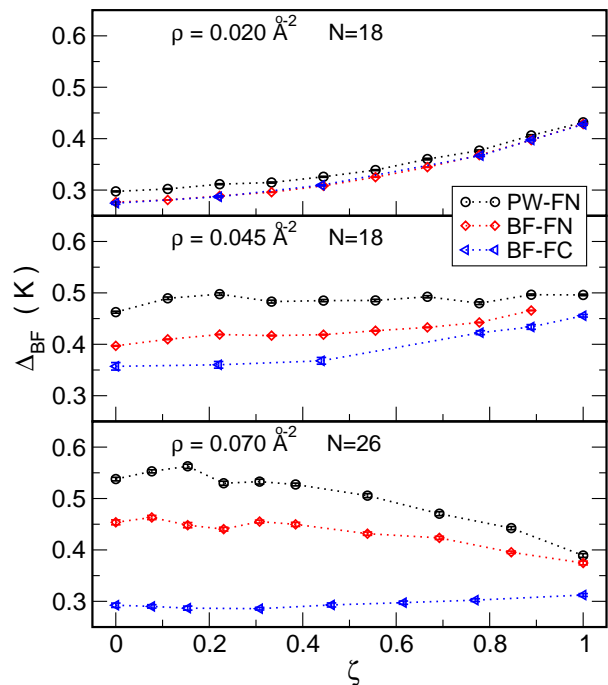


Figure 3: (Color online) Upper panel: Bose-Fermi gap,  $\Delta_{BF}$ , as a function of the spin polarization,  $\zeta$ , at density  $\rho = 0.020 \text{ \AA}^{-2}$  evaluated via PW-FN, BF-FN, and BF-FC with  $N = 18$  particles. Middle panel: Bose-Fermi gap,  $\Delta_{BF}$ , as a function of the spin polarization,  $\zeta$ , at density  $\rho = 0.045 \text{ \AA}^{-2}$  evaluated via PW-FN, BF-FN, and BF-FC with  $N = 18$  particles. Lower panel: Bose-Fermi gap,  $\Delta_{BF}$ , as a function of the spin polarization,  $\zeta$ , at density  $\rho = 0.070 \text{ \AA}^{-2}$  evaluated via PW-FN, BF-FN, and BF-FC with  $N = 26$  particles.

The statistical uncertainties are below the symbols size.

about  $0.002 \text{ \AA}^{-2}$ ; the ferromagnetic fluid is never stable. From the polarization energy we obtain a spin susceptibility enhancement in excellent agreement with the experimental values.

The need for an exact QMC approach is witnessed by the failure of the Fixed Node approximation with back-flow correlations to predict the lack of a polarization transition experimentally observed in the fluid phase, let alone an accurate value for the spin susceptibility.

The estimation of the Bose-Fermi gap via the Fermionic correlation method is limited to relatively small systems: the present results are obtained with either 18 or (in most cases) 26 particles. While the size effect remains the main source of uncertainty of the present calculation, the agreement of the calculated and measured spin susceptibility suggests that finite-size errors are relatively small.

## A. Acknowledgements

This work has been supported by CASPUR, Regione Lombardia and CILEA Consortium through a LISA Ini-

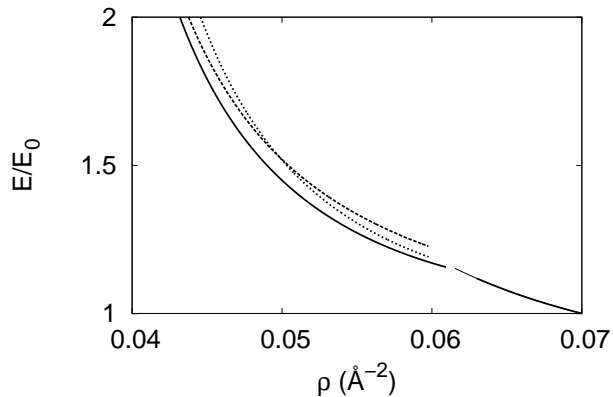


Figure 4: Unbiased FC versus Fixed-Node equation of state. Thick solid line (broken across the coexistence region): paramagnetic liquid and solid  ${}^3\text{He}$  (FC); dashed line: paramagnetic liquid (FN); dotted line: ferromagnetic liquid (FN); the dashed and dotted lines terminate at the FN freezing density; thin solid line: energy of the solid, down to the FN melting density. For each density, the energy is relative to the energy  $E_0$  of the mass-3 boson fluid.

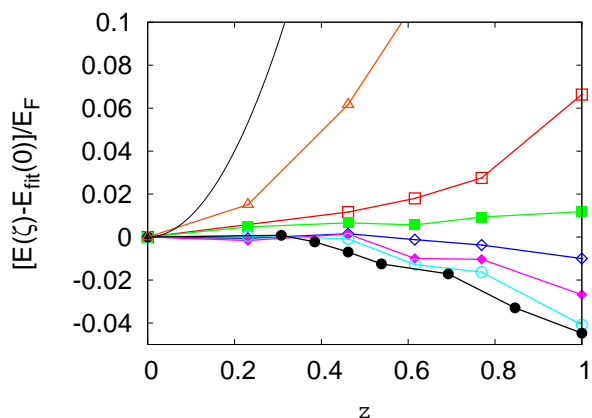


Figure 5: (Color online) Fixed-node results for the polarization energy  $E(\zeta) - E_{\text{fit}}(0)$  relative to the Fermi energy  $E_F$  at  $\rho = 0.020$  (open triangles),  $0.045$  (open squares),  $0.050$  (filled squares),  $0.055$  (open diamonds),  $0.060$  (filled diamonds),  $0.065$  (open circles),  $0.070$  (filled circles)  $\text{\AA}^{-2}$ , i.e. from top to bottom. The function  $E_{\text{fit}}(\zeta)$  is a quadratic polynomial in  $\zeta^2$  fitted to the simulation data; the solid line is the density-independent result for non-interacting particles.

tiative (Laboratory for Interdisciplinary Advanced Simulation) 2010 grant [<http://lisa.cilea.it>]

### Appendix A: GIFT algorithm variant

The inversion procedure that has been employed in this work is a variant of the GIFT algorithm<sup>27</sup>. This new algorithm puts together the idea of the falsification principle<sup>27</sup> and a modified implementation of the Prony's

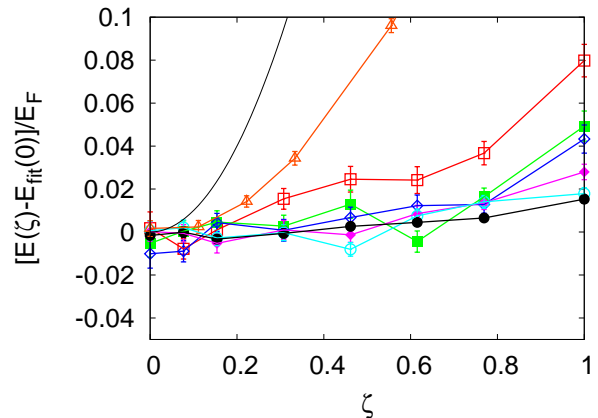


Figure 6: (Color online) Exact results for the polarization energy  $E(\zeta) - E_{\text{fit}}(0)$  relative to the Fermi energy  $E_F$  at  $\rho = 0.020$  (open triangles),  $0.045$  (open squares),  $0.050$  (filled squares),  $0.055$  (open diamonds),  $0.060$  (filled diamonds),  $0.065$  (open circles),  $0.070$  (filled circles)  $\text{\AA}^{-2}$ , in order of decreasing dispersion. The function  $E_{\text{fit}}(\zeta)$  is a quadratic polynomial in  $\zeta^2$  fitted to the simulation data; the solid line is the density-independent result for non-interacting particles.

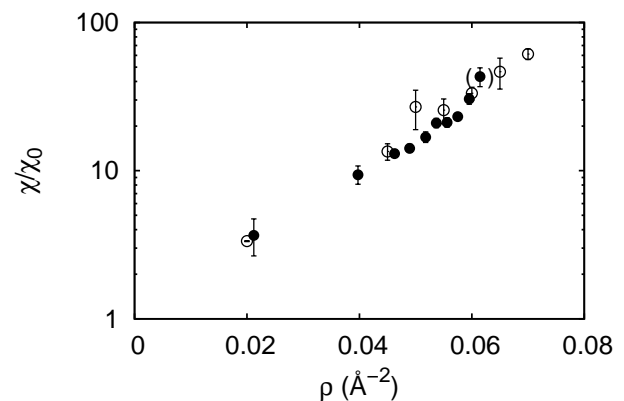


Figure 7: Enhancement of the spin susceptibility as a function of the density: (filled circles) as measured in the second layer of  ${}^3\text{He}$  on graphite<sup>2</sup>; (open circles) as calculated assuming a quadratic dispersion over the whole polarization range in Fig. 6. The corresponding Fixed-node result from Fig. 5 would diverge at  $\rho \simeq 0.050 \text{\AA}^{-2}$ .

method<sup>30</sup>, a non-iterative parametric technique for modeling using a linear combination of exponential functions. Starting from the basic relation in (12), which has the general form

$$f(\tau) = \sum_{i=0}^{\infty} s_i e^{-\omega_i \tau} \quad , \quad (\text{A1})$$

provided that we are allowed to truncate the previous series,  $\sum_{i=0}^{\infty} \rightsquigarrow \sum_{i=0}^{n-1}$ , the Prony's method is computationally very efficient (it runs in polynomial time) in deducing the coefficients  $\{s_i\}_{i=0}^{n-1}$  and  $\{\omega_i\}_{i=0}^{n-1}$  from a limited set of

estimations,  $f(k\delta\tau) = f_k^*$  at  $k = 0, 1, \dots, 2n - 1$  of  $f(\tau)$ , being  $\delta\tau$  the time step of the QMC simulation. The main steps of this algorithm are the following:

1. solve the regularized linear system

$$\mathbf{K}\mathbf{a} = \mathbf{b} \quad (\text{A2})$$

defined by the Henkel matrix  $K_{ij} = f_{i+j}^*$  and by the coefficients  $b_i = f_{n+i}^*$  ( $i, j < n$ )

2. find the roots  $\{z_i\}_{i=0}^{n-1}$  of the polynomial

$$z^n + a_{n-1}z^{n-1} + \dots + a_1z + a_0 \quad (\text{A3})$$

as eigenvalues of its respective companion matrix and obtain  $\omega_i = -\frac{1}{\delta\tau} \ln z_i$

3. solve the regularized linear system

$$\mathbf{A}\mathbf{s} = \mathbf{c} \quad (\text{A4})$$

defined by the Vandermonde matrix  $A_{ij} = z_j^i$  and by the coefficients  $c_i = f_i^*$  ( $i, j < n$ )

The transition from a nonlinear problem to two linear problems and one eigenvalues problem is the main characteristic of this algorithm; from a mathematical and computational point of view this is an advantage. Of course, the ill-posedness of this problem remains (our implementation uses the truncated singular value decomposition regularization) and some care is necessary to deal with instability against noise<sup>31</sup>. Such method fits the general scheme of the GIFT approach<sup>27</sup>, providing a very efficient alternative to genetic algorithms in the implementation of the falsification principle (when dealing with Laplace transform inversion).

- 
- <sup>1</sup> C. P. Lusher, B. P. Cowan, and J. Saunders, *Phys. Rev. Lett.*, **67**, 18 (1991).
  - <sup>2</sup> K.-D. Morhard, C. Bauerle, J. Bossy, Yu. Bunkov, S. N. Fisher, and H. Godfrin, *Phys. Rev. B*, **53**, 2658 (1996).
  - <sup>3</sup> A. Casey, H. Patel, J. Nyeki, B. P. Cowan, and J. Saunders, *Phys. Rev. Lett.*, **90**, 11 (2003).
  - <sup>4</sup> J. Boronat, J. Casulleras, V. Grau, E. Krotscheck, and J. Springer, *Phys. Rev. Lett.*, **91**, 8 (2003).
  - <sup>5</sup> H. Fukuyama, *J. Phys. Soc. Japan* **77**, 111013 (2008).
  - <sup>6</sup> Y. Matsumoto, D. Tsuji, S. Murakawa, H. Akisato, H. Kambara, and H. Fukuyama, *J. Low. Temp. Phys.*, **138**, 271 (2005).
  - <sup>7</sup> P. A. Whitlock, G. V. Chester and B. Krishnamachari, *Phys. Rev. B*, **58**, 8704 (1998).
  - <sup>8</sup> H. M. Bohm, E. Krotscheck, M. Panholzer, H. Godfrin, H. J. Lauter, M. Meschke, *J. Low. Temp. Phys.*, **158**, 194-200 (2010).
  - <sup>9</sup> F. H. Zong, C. Lin, and D. M. Ceperley, *Phys. Rev. E*, **66**, 036703 (2002).
  - <sup>10</sup> M. Holzmann, B. Bernu and D. M. Ceperley, *Phys. Rev. B* **74**, 104510 (2006).
  - <sup>11</sup> N. D. Drummond, R. J. Needs, *Phys. Rev. Lett.*, **102**, 126402 (2009).
  - <sup>12</sup> G. Carleo, S. Moroni, F. Becca, and S. Baroni, *Phys. Rev. B* **83**, 060411 (2011).
  - <sup>13</sup> P.J. Reynolds, D.M. Ceperley, B.J. Alder, and W.A. Lester, *J. Chem. Phys.* **77**, 5593 (1982).
  - <sup>14</sup> M. A. Lee, K. E. Schmidt, M. H. Kalos, and G. V. Chester, *Phys. Rev. Lett.* **46**, 728731 (1981); K. E. Schmidt and M. H. Kalos, in *Monte Carlo Methods in Statistical Physics II*, ed. K. Binder (Springer Verlag, Berlin, 1984).
  - <sup>15</sup> M. Caffarel and D. M. Ceperley, *J. Chem. Phys.* **97**, 8415 (1992).
  - <sup>16</sup> V. Grau, J. Boronat and J. Casulleras, *Phys. Rev. Lett.* **89**, 045301 (2002).
  - <sup>17</sup> R. A. Aziz, V. P. S. Nain, J. S. Carley, W. L. Taylor and G. T. McConville, *J. Chem. Phys.* **70**, 4330 (1979).
  - <sup>18</sup> M. Rossi, M. Nava, L. Reatto, and D.E. Galli, *J. Chem. Phys.* **131**, 154108 (2009).
  - <sup>19</sup> A. Sarsa, K.E. Schmidt and W.R. Magro, *J. Chem. Phys.* **113**, 1366 (2000).
  - <sup>20</sup> S. Baroni and S. Moroni, *Phys. Rev. Lett.* **82**, 4745 (1999).
  - <sup>21</sup> K. E. Schmidt, Michael A. Lee, M. H. Kalos, and G. V. Chester, *Phys. Rev. Lett.* **47**, 807 (1981).
  - <sup>22</sup> D. M. Ceperley and M. H. Kalos, in *Monte Carlo Methods in Statistical Physics*, ed. K. Binder (Springer, New York, 1979).
  - <sup>23</sup> C. Lin, H. Zong and D. M. Ceperley, *Phys. Rev. E* **64**, 016702 (2001).
  - <sup>24</sup> D. E. Galli and L. Reatto, *Mol. Phys.* **101**, 1697 (2003).
  - <sup>25</sup> For the bosonic crystal, the trial function is of the Jastrow-Nosanow form; see L. H. Nosanow, *Phys. Rev. Lett.* **13**, 270 (1964). For the fermionic crystal, the trial function is of the Jastrow-Slater form, with Slater determinants of Gaussians centered at lattice sites.
  - <sup>26</sup> E. Vitali, D.E. Galli and L. Reatto, *Series of advances in Quantum Many Body Theory* **11** (2008).
  - <sup>27</sup> E. Vitali, M. Rossi, L. Reatto and D. E. Galli, *Phys. Rev. B* **82**, 174510 (2010).
  - <sup>28</sup> D.E. Goldberg, *Genetic Algorithms in Search, Optimization and Machine Learning* (Addison-Wesley, 1989)
  - <sup>29</sup> R. A. Aziz, F. R. W. McCourt and C. C. K. Wong, *Mol. Phys.* **61**, 1487 (1987).
  - <sup>30</sup> A. M. Cohen, *Numerical Methods for Laplace Transform Inversion*, p. 116 (Springer)
  - <sup>31</sup> P. Barone, A. Ramponi, and G. Sebastiani, *Inverse Problems* **17**, 77 (2001).